Evaluation of the adhesion forces between dust particles and photovoltaic module surfaces

Rima J. Isaifan[1,2*], Daniel Johnson[1,3], Luis Ackermann[1], Benjamin Figgis[1], Mohammed Ayoub[1]

[1] Qatar Environment and Energy Research Institute, Hamad Bin Khalifa University, Qatar Foundation, P.O. Box 5825, Doha, Qatar.

[2] College of Science and Engineering, Hamad Bin Khalifa University, Qatar Foundation, P.O. Box 5825, Doha, Qatar.

[3] Centre for Water Advanced Technologies and Environmental Research (CWATER), College of Engineering, Swansea University, UK.

Soiling of Photovoltaic (PV) modules is a growing area of concern due to the adverse effect of dust accumulation on PV performance and reliability. In this work, we report on four fundamental adhesion forces that take place at the first stage of soiling process. These are capillary, van der Waal, electrostatic and gravitational forces. It is found that under high relative humidity, the adhesion mechanism between dust particles and PV module surfaces is dominated by capillary force, while van der Waal force dominates under dry conditions. Moreover, real field data for long soiling periods over solar panels in Qatar were investigated and resulted in proposing a novel modified sigmoid function that predicts a relative humidity inflexion value at which transition in the particulate matter deposition rate takes place from low to high values. Moreover, the effect of surface roughness was investigated by measuring adhesion force over clean glass versus substrates that are coated with in-house developed anti-dust titania thin films.

Keywords: adhesion · soiling mechanism· capillary force · dust particles· van der Waal · Qatar · Atomic Force Spectroscopy

*Corresponding author: Rima Isaifan; Qatar Environment and Energy Research Institute (QEERI), Hamad Bin Khalifa University (HBKU), Qatar Foundation, P.O. Box 5825, Doha, Qatar e-mail: risaifan@hbku.edu.qa

1. Introduction

Soiling, the accumulation of particulate matter on the exposed surfaces of solar collectors, is a growing area of concern due to the adverse effect of dust accumulation on solar system performance and reliability [1]. The efficient deployment of solar panels have grown substantially over the last decade, nevertheless, the influence of dust deposition on PV surfaces have played an important factor reducing PV efficiency in different locations and under different environmental conditions.

Dust and solid aerosols adhere with great tenancy to solid surfaces [2]. The bonding mechanism between dust and solar surfaces via several adhesion forces depends on the environmental conditions, dust characteristics, surface treatment and contact surface area [3]. The most common adhesion forces that dominates between dust and solar surfaces are capillary forces, van der Waal and electrostatic [2]. Gravitational forces are also significant when the particle size is greater than 500 μm [4][5]. Capillary forces have been studied between particles at the nano/micro scale and solid surfaces and were found to depend strongly on humidity [3][6]. Jones et al. [3] used atomic force microscopy (AFM) to investigate adhesion forces between glass and silicon surfaces as a function of relative humidity (RH) in the range of 5-90%. In addition, they studied the effect of surface treatment (hydrophilic vs. hydrophobic) and found that small hydrophilic contacts show a large and monotonic increase of adhesion with RH. Rabinovich et al. [6] reported as well that the adhesion behavior of fine powders (with sizes approximately less than 10 μm) is significantly affected by relative humidity since it is a critical parameter that affects the magnitude of the attractive forces between the particle and the surface. Moutinho et al. [7] recently reported on two fundamental adhesion mechanisms to better understand and quantify soiling rates on solar panels; van der Waal and capillary adhesion

forces. They measured capillary forces in a stable environment created inside the AFM with RH ranging from 18 to 80%. Moreover, they investigated the effect of particle size and surface roughness on the adhesion bonds. They found that at lower relative humidity values, the adhesion mechanism is dominated by van der Waal forces, while at higher RH, capillary forces dominates since the water layer becomes thick enough to overcome the surface asperity. In addition, they reported that the surface roughness played a critical role in the adhesion strength. They found that when surface roughness increases, it reduces the contact area between the particle and surfaces and hence substantially decreases adhesion forces.

Several techniques have been developed to clean solar panels to mitigate the effect of soiling including the use of water, mechanical brushing, the use of surfactant and thin film coatings. Titanium dioxide thin films are the most popular hydrophilic material studied for self-cleaning applications [8][9]. Self-cleaning using TiO_2 films involves two stages; first, a split of organic dirt via photocatalytic process in the presence of ultraviolet light, and second, the diffusal of water to the whole surface instead of getting together due to the hydrophilicity of TiO_2 and hence rinsing the dust.

Recently, Quan et al. [10] have reported on a cost-efficient and simple approach synthesis of transparent coatings with different hydrophobicity for anti soiling applications. They designed four experiments to simulate the surface-dust interactions, one of which is a dust impinging experiment and the other three are dust removal experiments which all were tracked via a high-speed camera to capture the impinging and depositing process of dust driven by air stream. They found that different moving behaviors of dust particles can be observed on the bare and coated glass surfaces, which can be used to illustrate the different soiling phenomena. It was also found

that the low surface energy and rough structures of coatings work together to lower the adhesion forces between the particles and surfaces.

Moreover, various surface modification technologies have been used to develop superhydrophobic surface, however their durability has been recognized as the major obstacle for the real applications. Zhi et al. [11] recently reported on a quantitative investigation to evaluate the effects of different surface modification methods (suing four low surface energy chemicals) on the surfaces' mechanical durability over superhydrophobic surfaces prepared by the combination of two surface roughing methods (etching and sandblasting). They used XPS to analyze the elements composition and AFM to measure the roughness of the surfaces. The durability of these surfaces was tested by a sandpaper abrasion experiment. The results showed that the low surface energy materials had significant effects on the surface roughness, which would then play an important role in the durability of these rough surfaces.

In this work, the adhesion forces between dust particles and glass surfaces are evaluated by estimating the four main forces that control the adhesion mechanism at the early soiling phase. The evaluated forces are: capillary, van der Waal, electrostatic and gravitational forces. Moreover, the effect of humidity is further investigated by studying real field data collected at our Solar Test Facility for long periods of soiling time without cleaning. A novel approach has resulted in proposing a modified sigmoid function that predicted a relative humidity inflexion value at which particulate matter deposition transition takes place from low to high rate. To this end, the effect of surface roughness and the adhesion force between dust particles on TiO_2-coated films, developed in house, are investigated via measurements using AFM. The measured values are compared with adhesion forces over uncoated glass substrates as a reference sample.

2 Experimental

2.1 TiO_2-coated films preparation

TiO_2 nanocolloids were prepared by polyol method as detailed elsewhere [12][13][14]. In brief, 125 mL of tetraethyleneglycol (TEG) (Sigma-Aldrich, ≥ 99%) were measured and poured in a three-neck flask. Then, 2.7 g of titanium (IV) oxysulfate $TiOSO_4$ (Sigma-Aldrich 99%) precursor salt were measured and introduced into the three-neck flask and stirred for 30 min to dissolve in the TEG at room temperature. The mixture was mechanically stirred and heated at a rate of 6^{o} C min^{-1} from room temperature to 165 ^{o}C under reflux for 3 hours. At this stage, TiO_2 nanocollids were synthesized.

To prepare the coated samples; borosilicate plate glass slides (Chemglass CG-1904-36) of 25 mm x 10 mm x 2 mm (width x length x thickness) were used as work pieces. Before deposition, the glass substrate samples were properly cleaned with Piranha solution, ethanol, rinsed with deionized water and left to dry in the oven at 70 ^{o}C for 30 minutes. The dried glasses were then dipped in the prepared TiO_2 nanocolloids for 2 hours at 20 ^{o}C and at a relative humidity of around 30 %. The samples were then placed in an oven (Thermolyne, Thermo Scientific) at a temperature of 400 ^{o}C under air for 2 hours [9].

2.2 Characterization techniques

Nine bulk dust samples have been collected around urban Doha in the winter during December 2016 including samples from The Solar Test Facility. The size distribution of the samples was characterized via optical microscope where optical images were taken and the particle size of about 300 particles was measured in each image. The chemical composition of the PM samples was performed via SEM/EDS model JCM-6000PLUS NeoScope Bench top. This instrument employs two different types of detectors which are secondary and back scattered electrons detectors. In this study, Secondary Electron mode was used to acquire an image of the

cross sections under study with a high magnification and resolution. This type of detectors was selected because the cross section illuminates shorter wavelength associated with the electrons to attain high magnification. According to Goldstein et al. [15] the resolution is determined as a function of the density which depends on the penetration of the electron beam to a certain depth in a sample. The mass concentrations of 10 elements (Al, Ca, Na, Mg, Cl, Fe, K, S, Si, Ti) were determined for each sample.

AFM force interaction measurements were carried out using a Dimension Icon model AFM with NanoScope V Controller (Bruker AXS, USA). All measurements were made in ambient conditions using NP-O type silicon nitride tip-less contact mode probes (Bruker, USA). Single dust particles were mounted close to the apex of the probe using careful control of the AFM stage. Firstly, a thin smear of slow curing epoxy resin was placed on the end of a cleaned glass microscope slide. A small amount of dust particles was placed elsewhere on the same slide. Excess particles were removed using a stream of nitrogen to leave only individual particles directly attached to the surface. The tip of the AFM cantilever was first placed into the edge of the epoxy resin, taking care to only remove a thin layer of adhesive. Next, an individual particle separated from other particles of suitable size and regular shape was identified. The probe tip was then brought into and out of contact with the particle. Colloidal probes created in this manner were left overnight to allow the adhesive to fully cure. For each set of measurements, 100 particle – surface interaction events were recorded, with each measurement being part of a 10 x 10 array separated by 1 μm in the *x* and *y* directions, to ensure that all measurements were taken from different locations on the sample surface. From features of the force distance curves the adhesion force for each interaction was measured and mean values for each surface of interest were calculated [16][17].

The surface wettability was evaluated by measuring the contact angle of deionized water droplets deposited on the film surface under ambient conditions using rame-hart with three replicates. The acquired images have been elaborated with Drop Image software to obtain the average contact angles.

2.3 Photovoltaic module soiling field measurements

Field measurements of PV soiling were made at the Solar Test Facility in Doha, Qatar. Three PV systems were used, each comprising of a string of eight polysilicon modules tilted South at 22°. Module back-surface temperature and DC power of each system were measured and logged every minute. DC power measurements were corrected to the STC temperature of 25 °C using the module's stated power temperature coefficient. From these temperature-corrected power measurements (refer to eqn. 1), daily energy yields at 25 °C ($EY_{25C,}$ units W·h) of the arrays were calculated, and normalized by daily plane-of-array irradiation (GPOA, units $W \cdot h \cdot m^{-2}$) and array installed capacity (W_p, units W). This quantity was the temperature-corrected Performance Ratio (PR, units $W^{-1} \cdot m^2$) for the day as per eqn. (1):

$$\boldsymbol{PR_i = \frac{EY_{25C,i}}{GPOA_i W_p}} \qquad \textbf{(1)}$$

where *i* the day number.

Finally, the PR values of the three arrays were averaged. Note that even when the array is perfectly clean, PR is not necessarily unity. From four years of test data it was found that average PR of a cleaned array was around 0.9.

3 Results and discussion

3.1 Characterization of dust

Figure 1 shows representative SEM micrographs of dust particles taken at different magnifications. The micrographs show different sizes and morphologies of dust particles.

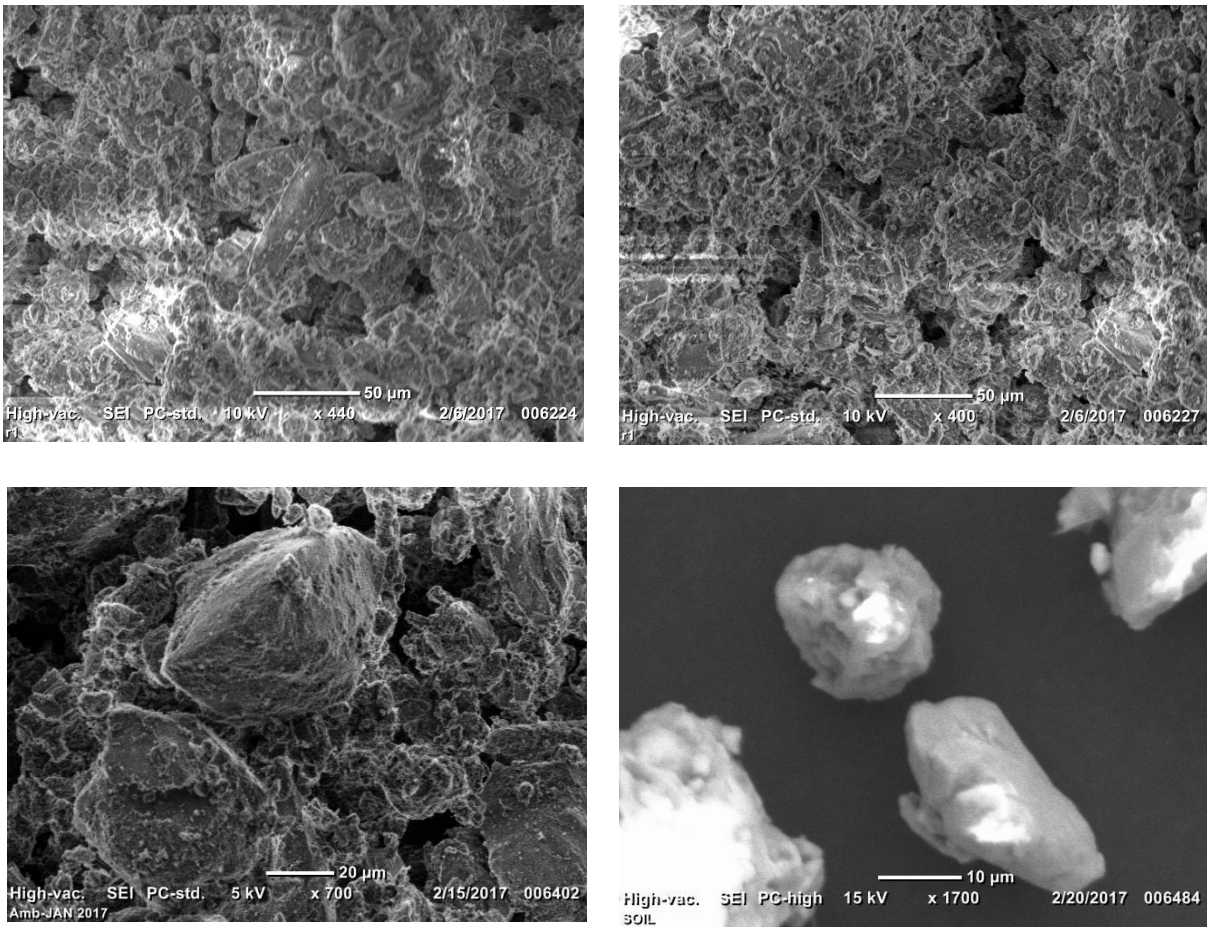

Figure 1. Representative SEM micrographs with various magnifications of the dust particles collected at the Solar Test Facility.

The size distribution of the particles (Fig. 2) was found to be in the range of 1-100 µm with an average particle size of 7.38 µm. The particles show different morphologies with some agglomeration under humid conditions.

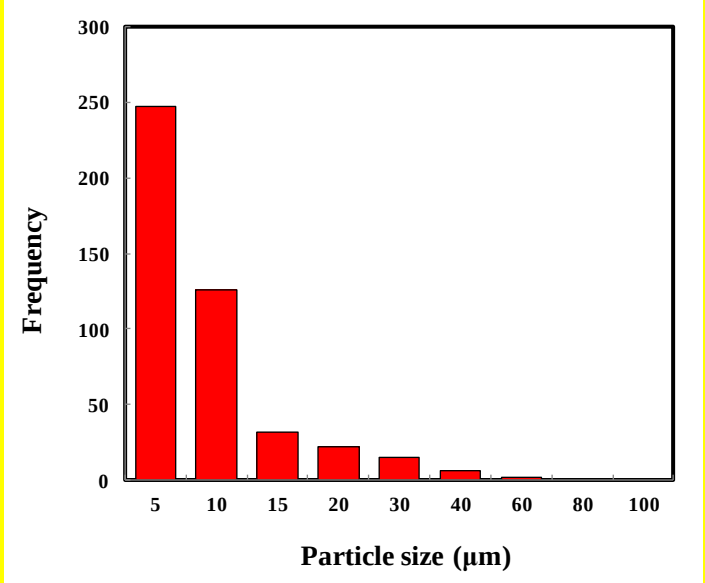

Figure 2. Particle size distribution of the dust samples considered in this study.

The mass concentration of elements in order from greatest to smallest are Ca, Si, Fe, Mg, Al, Ti, K, Na, S and Cl. This elemental composition is found to be similar to the composition reported earlier by another study on dust samples collected in Qatar [18][19][20]. It is of critical importance to identify the major components in the dust sample as it will indicated the value of Hamaker constant to be used to evaluate van der Waal forces as will be shown later.

Table 1. Detected elemental species (mass %) in the dust samples.

Element	Na	Mg	Al	Si	S	Cl	K	Ca	Ti	Fe
Mass %	4.0	8.3	7.2	26.2	2.2	1.5	5.3	32.0	6.9	11.7

3.2 Evaluation of adhesion forces

At the initial adhesion stage in the soiling process between dust particles and surfaces, the adhesion of dust particles on solid surfaces is governed by several forces including capillary forces, van der Waal, electrostatic and gravitational [4][21][22]. For small particles (radius < 500

μm), the gravitational force is negligible [5][4][23]. Nevertheless, it will be evaluated and compared with other dominant forces in this work.

3.2.1 Capillary adhesion

Adhesion by capillary forces is dominant when moisture is present in the surrounding environment (Fig. 3). Moisture causes the particles to adhere to the surface through capillary action. When capillary condensation is present, water starts to condense onto clean glass surface at relative humidity (RH) well below the dew point due to the presence of small crevices causing the creation of tightly curved concave meniscus [3]. Therefore, the capillary force is a combination of two force components, F_{st} which is the force due to surface tension and F_{mc}, the force due to the difference in pressure between air and the water meniscus [7][24].

The capillary force is proportional to the particle diameter and is significant especially for larger particles (diameter over 10 microns) [22]. This effect is evident in particle adhesion on glass surfaces for which the adhesion force tend to increase slowly with RH until a critical threshold is reached, typically around 60 - 70% RH, and then increases rapidly [21][22][25]. The capillary forces between a spherical particle and a flat surface is normally given by the following equation, [26]:

$$F = 4 \pi R \gamma \cos \theta \qquad (2)$$

Where R is the radius of the spherical dust particle (R= 3.69 µm in our samples), γ is the surface tension of water –air at the experimental conditions and θ is the contact angle of water on the substrate. This equation, although used extensively in literature to estimate the capillary force ideally between smooth sphere adhered to a smooth flat substrate, has no dependence on the relative humidity which is the main factor that affects capillary forces and, consequently, should have a fixed value even at 0% RH. Experimentally, it was proven that there is a critical effect of

relative humidity, therefore, there must be a value of RH at which capillary forces first start to appear and below which they are absent. To account for this problem, there were two approaches in literature. The first was suggested by Coelho and Harnby [27] which was based on the assumption of thermodynamic equilibrium between the liquid meniscus, bulk liquid in the annulus and vapor. The critical values of relative humidity, obtained within this framework, were in the order of 70-99% RH. The second approach to encounter for the critical humidity was suggested by Rabinovich et al. [6] based on the proposal that there is certain annulus volume or dimension, below which, the adsorbed molecules cannot be considered a macroscopic phase and, consequently, no surface tension or capillary force would exist at humidity less than that critical value. Rabinovich et al. [6], after analysis of literature data detailing force measurements in addition to their own experimental data, found that the critical radius of the meniscus corresponded to approximately 1 nm.

Hence, at zero or low humidity, only a thin mono-molecular film exists on the surface which cannot form a meniscus, then as RH increases, a critical value will be reached above which the capillary force will act in addition to van der Waal forces (dry adhesive forces) until it dominates the adhesion mechanism. This interesting consideration is in agreement with the fact that when the meniscus forms, the magnitude of van der Waal forces for solids through water is significantly less than in air [6][28][29][30]. For instance, Hamaker constant for calcite interacting through water is 1.03×10^{-20} J , which is eight times less than the Hamaker constant of calcite interacting through air, 8.45×10^{-20} J [6][31]. Therefore, it was suggested in several works that the contribution of van der Waals force at high relative humidity should be neglected [6][7] [30].

Accordingly, Rabinovich et al. [6] has modified eqn. (2) to include the effect of the relative humidity inherently in *r* as per the following equation:

$$Fc = 4\pi R\gamma \cos\theta\,[1 - z/(2r\cos\theta)] \quad (3)$$

Where *R* is the particle radius, γ is the surface tension, *z* is the separation distance (0.4 nm), θ is the contact angle and *r* is the equilibrium radius of meniscus which is given by Kelvin's equation [6] :

$$r = -\frac{V\gamma}{N_a k T \ln(\frac{P}{P_S})} \quad (4)$$

Where *V* is the molar volume of the liquid (in this case water, V = 18.03 ml· mol^{-1}), γ is the surface tension of the liquid, *Na* is Avogadro's number (6.022 x 10^{23} atom · mol^{-1}), *k is* Boltzmann's constant (1.38 x 10^{-23} m^2· Kg ·s^{-2}· K^{-1}) and *T* absolute temperature (K), P/P_S is the relative humidity.

The average temperature when the samples were exposed to dust was 29°C (302 K) and the average relative humidity was 72%. The tabulated data of the water –air surface tension (γ) at these conditions is 71.2 x10^{-3} N·m^{-1} [31].

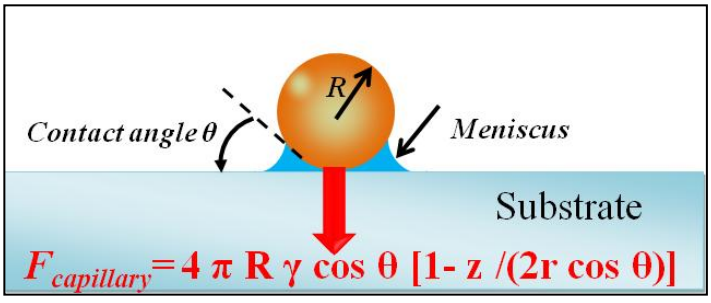

Figure 3. Representative scheme of the capillary force between dust particle and glass substrate.

Based on this, Kelvin radius was estimated using eqn. (4):

Kelvin radius = 1.56 nm (it is noticed this value is well above the critical Kelvin radius of the meniscus (about 1 nm) below which no capillary forces would exist [6].

Hence, the capillary forces are calculated using eqn. (3) and found to be, **Fc= 1951 nN.**

Table 2 shows the capillary force calculated under our conditions at relative humidity range from 10% to 99%.

Table 2. Capillary forces calculated at relative humidity in the range of (10-99%).

Relative Humidity (%)	Capillary Force (nN)
10	-570
20	309
30	837
40	1207
50	1500
60	1737
70	1934
80	2109
90	2262
99	2270

3.2.2 van der Waals (VDW) force:

London-van der Waal (dispersion) force (Fig. 4) is the force by which any atom or molecule is attracted by any other atom or molecule [2][32]. In general, under dry and electrically neutral ambient conditions, the van der Waal force can be considered to be the most dominant adhesion force between the particles and solid surfaces [4][33]. Nevertheless, the work presented in this paper is related to the adhesion of dust particles onto glass substrates when left to deposit for a

week under an average temperature and humidity of 29°C and 72%, respectively. These conditions are humid and hot which makes the capillary force to be dominant as shown earlier.

The van der Waal force between a spherical particle and a flat surface can be expressed by the following equation [29][34]:

$$F_{VDW} = \frac{A\,R}{6z^2} \qquad (5)$$

Where A is Hamaker constant, R is the particulate's radius and z is the separation distance between the particulate and the flat substrate. The Hamaker constant reflects the strength of van der Waal force and depends on the type of materials of the particulate and the substrate in the medium of contact. Hence, the elemental composition of dominant material in the dust particles is of paramount importance to determine the Hamaker constant of the material under study.

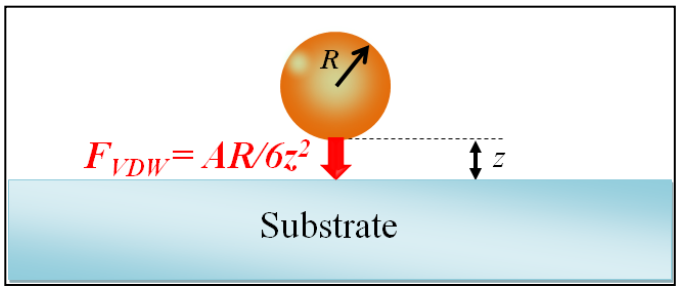

Figure 4. Representative scheme of van der Waal force between dust particle and glass substrate.

Where most dust particles in desert areas are made up of silica, the particulate matter in Qatar have been extensively studied and found to contain more calcite due to the nature of the soil in this region [1][35] (Table 1). In this work, Hamaker constant is taken as 1.03 x 10^{-20} J for the system of calcite spherical particle in contact with glass substrate in water and 8.45 x 10^{-20} J in air [31], and the separation distance is taken as 4 A^o [4][36]. Hence,

F_{VDW} = **39.4 nN** and **324 nN** in humid and dry air, respectively.

Eqn. (5) assumes an ideal situation where the particle and surface are both smooth, therefore z (the distance between the particle and the surface) takes a value in the range of 0.35-0.4 nm [4] [7][36]. In the case of surfaces with nanoscale roughness, the minimum height z can be adjusted to encounter for the roughness of the surface.

Hence;

z = 1.817 x Roughness RMS (nm) [6] **(6)**

Table 3 shows a comparison between adhesion forces calculated over ideal smooth surface and compared with forces over coated and uncoated substrates based on their modified surface roughness.

Table 3. Theoretical adhesion forces of dust particles over TiO_2-coated and uncoated glass substrates vs. ideal smooth surfaces.

Case	**Ideal (smooth surface)**	**Uncoated sample**	**TiO_2-Coated sample**
Roughness RMS (nm)	Smooth	0.65*	3.30*
z (nm) [eq. 6]	0.35-0.4 [4] [7] [36]	1.18	5.99
Adhesion force in humid air (nN)	*39.40*	*4.69*	*0.18*
Adhesion force in dry air (nN)	*324.00*	*37.11*	*1.44*

***Values are measured experimentally in this work via AFM.**

The italic font indicates theoretical estimates as per eqn. (5).

3.2.3. Electrostatic force

Dust particles in the atmosphere may acquire electric charge through collisions or other means. Even if the PV module surface is not (beforehand) charged, the charged particle will

attract opposite charges on it giving rise to an image charge on the surface (Fig. 5) which induces a coulomb force, i.e. involving permanent charges of opposite sign [22].

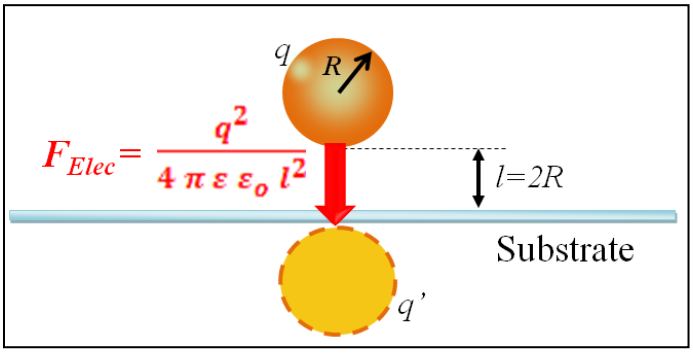

Figure 5. Representative scheme of the electrostatic force between dust particle and glass substrate.

On non-conductive materials such as glass, surface charges can as well appear via tribo-electrification with unpredictable level of charges [37]. Tribo-electrofication effect is a type of contact electrification in which certain materials become electrically charged after they come into frictional contact with different materials. The interaction force due to this charge distribution is given by eqn. (7) to evaluate electrostatic force [38][39][40]:

$$F_{electrostatic} = \frac{q^2}{4 \pi \varepsilon \varepsilon_o l^2} \quad (7)$$

Where q is the charge of dust particle (C), ε is the dielectric constant of the medium between the particle and the surface (for air, ε=1), ε_o is the permittivity of the free space medium (air in this case) and l is the separation distance between the charge centers which is approximately equal to 2R, where R is the radius of the particle [38]. The average charge of the dust particle was reported by Deputatova et al. [41] for different masses of dust particles. Accordingly, the experimental measurements of Deputatova et al. [41] was extrapolated to find the charge of the dust particle in our study based on its average mass. To obtain the average mass of our dust

particles, the density of the dust sample was measured and found to be 882.7 Kg/m^3, hence the average mass of dust particles in our study is 1.85 x 10^{-13} Kg which yields an average particle charge of 2.5 x10^3 ē [41]. This value should be converted to coulomb (1 ē = 1.602 x 10^{-19} C) to be used in eqn. (7), hence q= 4.0 x10^{-16} C. The permittivity of air is 8.85x 10^{-12} C^2 ·N^{-1}·m^{-2} [42] and R is the particle radius (3.69 µm).

Hence, the electrostatic force $\boldsymbol{F_{electrostatic}}$**= 0.026 nN**

3.2.4. Gravitational force:

The gravitational force (Fig. 6) between spherical particle and a substrate is given by eqn. (8):

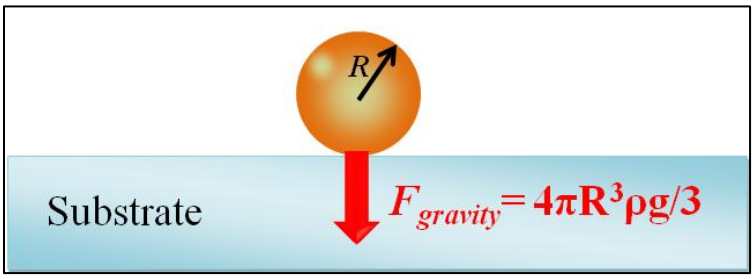

Figure 6. Representative scheme of gravitational force between dust particle and glass substrate.

$$\boldsymbol{F_{gravity} = \frac{4\pi R^3 \rho g}{3}} \qquad \textbf{(8)}$$

Where R is the particulate radius, ρ is the density of the particulate's material (measured to be 882.7 Kg/m^3 for our dust sample) and g is the gravitational acceleration constant.

Hence, $F_{gravity}$ = 1.8 x 10^{-12} N = **0.0018 nN**

The results show that the capillary force accounts for 98% of the forces acting on the particle-surface attraction mechanism, while van der Waal accounts for 2% under the humid environmental conditions. On the other hand, the gravitational force is negligible compared with the other three forces as expected for particles with diameter less than 500 µm [5][4][23]. The electrostatic force is as well negligible which is in agreement with previous studies of similar

conditions [7][27][30]. Visser [27] stated that the humidity greatly reduces the effect of electrical forces. This is because when moisture is present, it will eliminate coulomb attraction by providing a path for dissipation (leakage) of the charges, even in low humidity environment [43] [44]. Another reason is that the image forces are inversely proportional to the dielectric constant of the surrounding medium, hence they are 80 times weaker in water than in air [45]. In addition, taking into consideration that glass substrate is non-conductor, the surface will tend to dissipate any near charges caused by the deposition of charged dust particles [34]. Therefore, the electrostatic adhesion force can be significant when charged dust particles deposit on PV surfaces under dry environmental conditions, contrary to the weather in The State of Qatar where high humid weather dominates mostly all over the year.

It is worth noting that there are several factors that would impact the first stage of soiling over PV. Figgis et al. [46] have recently investigated the effects of four parameters that impact condensation on soiled surfaces: relative humidity, surface–dew point temperature difference between the surface and the surrounding air, hygroscopic dust content that tends to absorb moisture from the air, and surface wettability (hydrophilic vs hydrophobic). The work utilized several natural and synthetic dust mixtures of various compositions which were studied via water adsorption isotherms, x-ray diffraction (XRD), ion chromatography and optical microscopy, on hydrophilic and hydrophobic surfaces, in the lab and field. It was found that water uptake by surface dust was strongly dependent on its content of hygroscopic material, and such material allowed microscopic condensation droplets to exist on a soiled glass coupon even when it was significantly warmer than the dew point.

3.3 Effect of relative humidity by field measurements of PM soiling on PV panels

In order to further investigate the effect of relative humidity on the extent of PM soiling on PV panels in Qatar, the cumulative effect of PM deposition was weighted against ambient RH. For this purpose, the daily performance ratio (PR as defined in the methodology section above) at the Solar Test Facility over 18 months was used (location shown in figure 7 with a red dot). The meteorological and air quality conditions were measured by the Air Quality Measuring Station (AQMS) of Qatar Environment and Energy Research Institute (QEERI).

Figure 7. Red dot shows the location of the Solar Test facility where PM soiling on PV panels data was obtained. Red circle shows a 1 km radius from the Solar Test facility. Highly transited roads are highlighted in yellow.

In order to properly correlate soiling with atmospheric conditions (more specifically with the relative humidity RH), long periods of continuous soiling that extend well beyond a month without cleaning or rain, were selected. PM with aerodynamic diameter of 10 micrometers (PM_{10}) was used for the analysis and measured using the BAM technique. The PM instrument

has a USEPA PM_{10} sampling head. This head has an aerodynamic impact plate to filter out particles with aerodynamic diameter larger than 10 µm. After particles larger than 10 µm have been filtered, then the air sample passes through a fiber glass filter paper where the particulates are collected and the total hourly PM_{10} loading is measured by the absorption of beta radiation from a sealed source (Carbon 14) by the sample accumulated within one hour. PM_{10} was transformed to Accumulated PM_{10}, defined as the sum of the PM_{10} concentrations since the last cleaning, with the reasoning that the soiling in the surface of the panel is also the accumulated effect since the last cleaning or rain event took place.

The accumulated PM_{10} and PR showed some correlation; but with a poor fit as shown in figure 8A. Further analysis and exploration of the data showed a relationship with RH, illustrated in figure 8B where distinct RH groups can be observed.

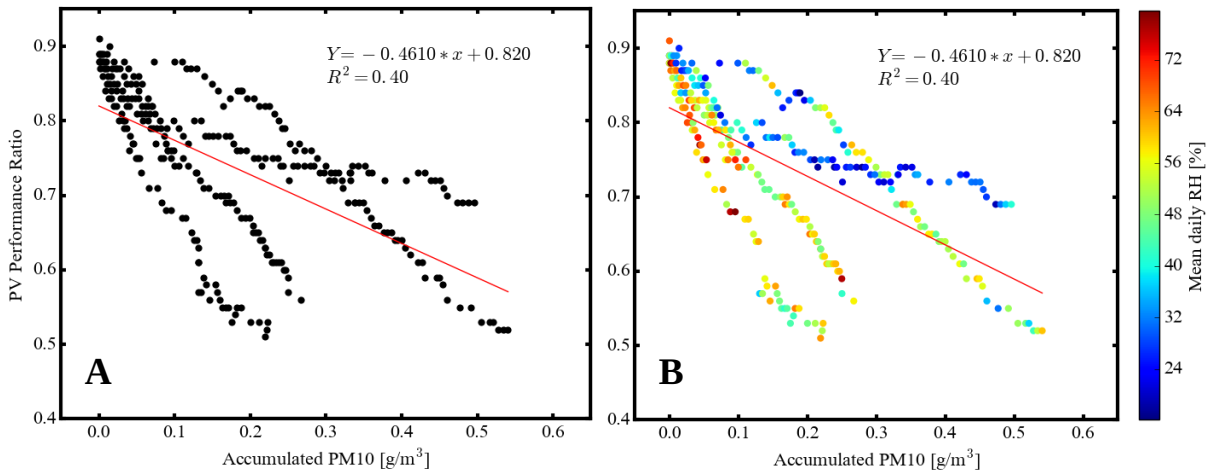

Figure 8. Panel A shows the correlation of accumulated PM_{10} and PV Performance Ratio, while panel B shows each data point colored by the daily mean of RH.

This apparent relationship with RH implies that only a fraction of the PM_{10} in the air would deposit on the PV panel, and this fraction is dependent on the RH at the time of deposition. This

fraction of PM_{10} will be denoted in this work as "sticky-fraction$_{(RH)}$" (since this will be the portion of the PM that adheres to the panel). The sticky-fraction$_{(RH)}$ was calculated using the following equation which is a modified sigmoid function.

$$\text{Sticky-fraction}_{(RH)} = [1 / (1 + (e^{(\text{Slope} * (\text{RH} + \text{RH inflexion}))})) * (1 - \text{Max deposition} - \text{Dry deposition})] + \text{Dry deposition} \quad \textbf{(9)}$$

Where, RH inflexion is the relative humidity where the deposition transition takes place from low to high rate. The slope is the gradient of the transition between low and high deposition rates. Dry deposition is a minimum ratio that will deposit onto the panel, independent of RH and Max deposition is a maximum percentage that will deposit onto the panel, independent of RH (Fig. 9).

Various methods to calculate the PM_{10} sticky-fraction using RH were tested, with a semi-step function producing the best fit for the data as shown in fig. 9.

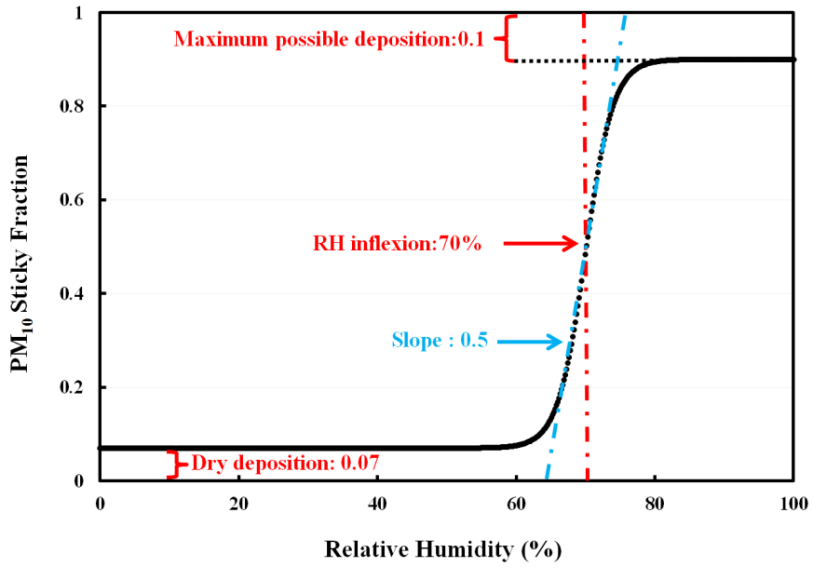

Figure 9. Value of the sticky-fraction as a function of RH, the values resulting in the best fit when compared to PV Performance Ratio are shown.

Upon weighting PM_{10} by the RH, multiplying PM_{10} times the sticky-fraction, the correlation between sticky PM_{10} and PR improved tremendously, as shown in figure 10, with an $R^2 = 0.94$.

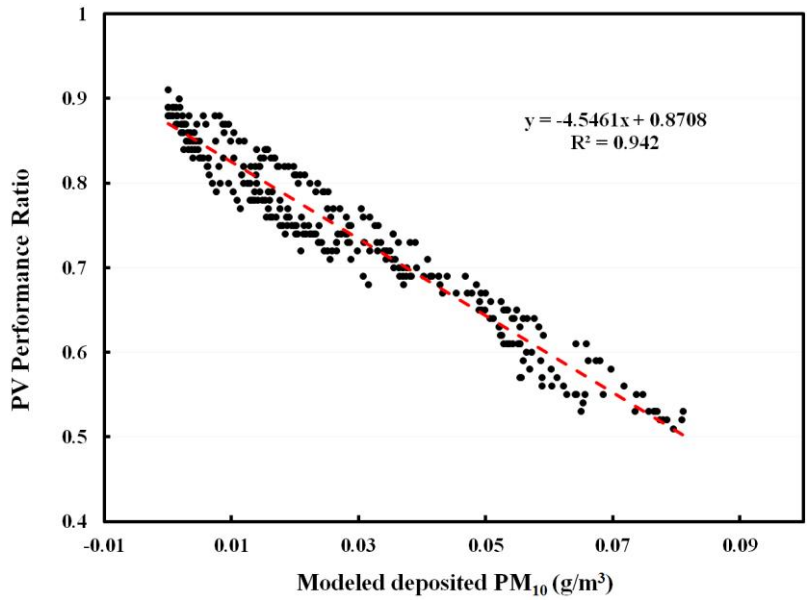

Figure 10. The final correlation between sticky PM_{10} and Performance Ratio.

Since the variability of PM_{10} is fairly low, it was found that the RH modulation was highly responsible for the PV soiling; furthermore, since the relationship to RH is non-linear with an inflexion point at 70%, a strong diurnal variability is predicted (see figure 11). From this prediction, it is calculated that about 70% of soiling occurs during the night, with the highest mean hourly soiling percentage at sunrise which is in agreement with the theoretical works reported earlier [7][21][22][25][27].

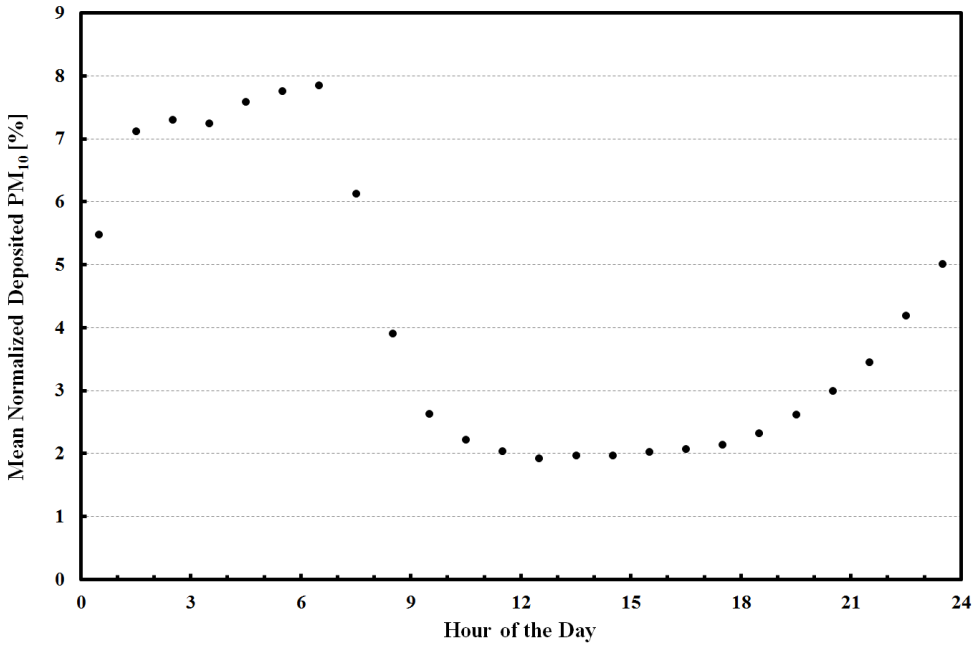

Figure 11. Diurnal variability of mean normalized deposited PM_{10}.

3.4 Adhesive force measurement by AFM

In an effort to mitigate dust deposition on PV modules under local desert environment, we have reported recently on an efficient and easy to scale up TiO_2 thin films which have improved self-cleaning properties [9]. The films which had an average thickness of 76.2 nm and refractive index of 1.51 showed distinctive anti soiling properties under desert environment resulting in 56% reduction of dust deposition rate over the coated surfaces compared with bare glass substrates after 7 days of soiling. Moreover, the transmission optical spectra of these films collected at normal incidence angle show high anti-reflection properties with the coated substrates having transmission loss of less than 6 % compared to bare clean glass [9].

The contact angle was measured (Fig. 12) over the coated surfaces and was found to be around 43^{o} in agreement with with what was reported earlier for anatase TiO_2 thin films deposited on glass substrates [47][48][49].

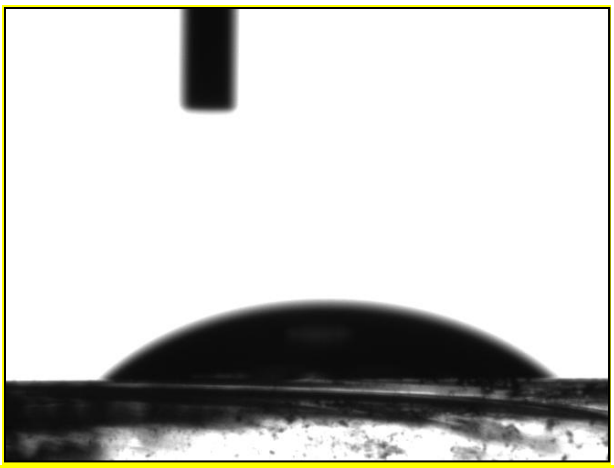

Figure 12. The contact angle measured over the coated glass surface.

The surface roughness of the coated and uncoated surfaces was measured (Fig. 13).

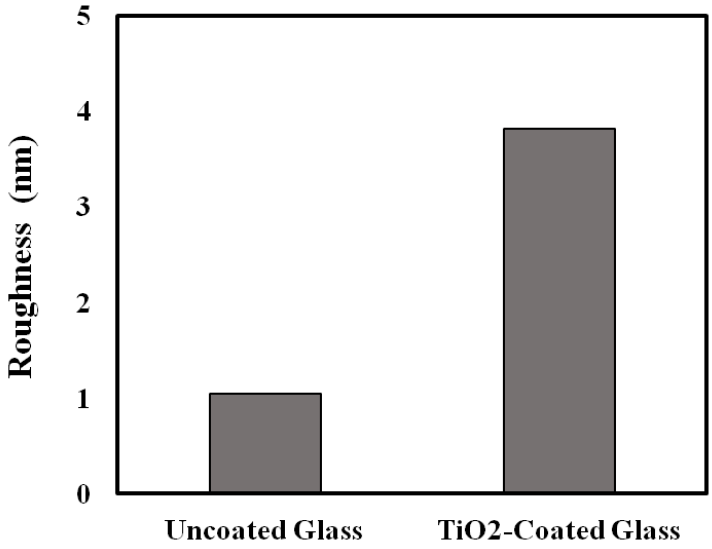

Figure 13. Surface roughness (RMS) of uncoated and TiO_2-coated substrates.

The average surface roughness of the coated samples was 3.3 nm which is 5 times greater than the surface roughness of the uncoated glass (0.65 nm). The surface roughness has a critical impact on the adhesion force between particles and substrates [50][51]. In general, as the surface roughness increases, the adhesion force decreases. This trend has been reported in several studies [3][6][7]. The effect of roughness has an impact mainly on the capillary force since the increase

of surface roughness prevents the formation of a complete capillary meniscus at the particle contact point and hence weakens the capillary force.

In order to investigate the validity of the estimated adhesion forces obtained in the above sections, the adhesion forces were measured experimentally via AFM (Fig. 14) between dust particles and the coated substrates under lab environmental conditions (T= 20^{o}C and RH = 30%) and were compared with adhesion force measured over the uncoated glass.

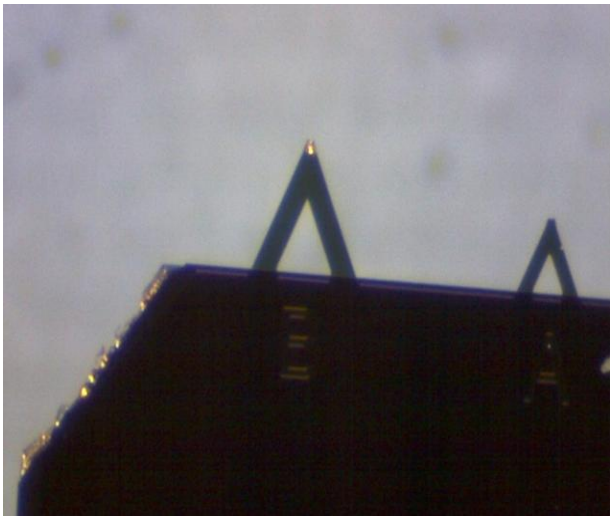

Figure 14. AFM tip with dust particle mounted for adhesion force measurement.

The experimental results to measure the adhesion force with AFM indicate an average adhesion force of 17.4 nN for the coated glass vs. 19.3 for the non-coated glass (Fig.15).

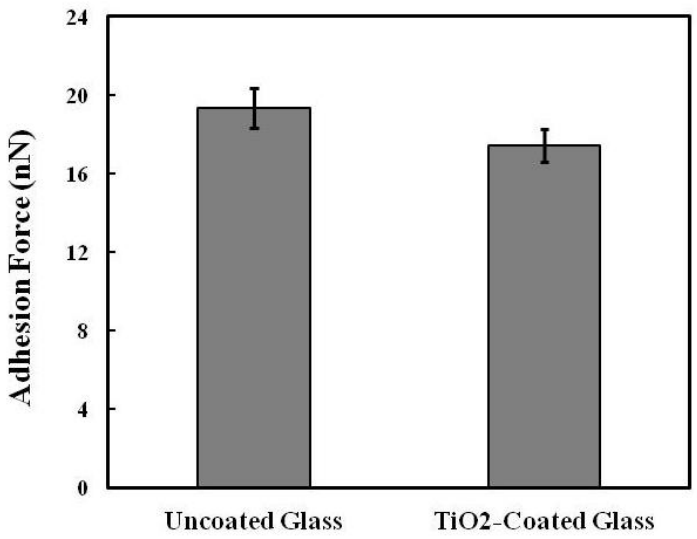

Figure 15. The average adhesion force between dust particles and coated and uncoated substrates.

These results indicate that under the lab relatively dry conditions (T= 20^{o}C and RH= 30%), the dominant adhesion force is van der Waal. Nevertheless, the effect of roughness was not pronounced in terms of reducing the adhesion force when comparing between the coated vs. uncoated glass since it would mainly affects capillary force where the conditions in the lab favors van der Waal.

It is worth mentioning that our results are dependent on the natural dust accumulated on PV solar panels which are mainly composed of calcite as indicated earlier. Nevertheless, several researchers studied natural and artificial dust particles and their influence on adhesion over glass surfaces as well as other surfaces. Tan et al. [34] reported on the adhesion of two different particles of similar sizes (dust and activated carbon) over different indoor surfaces including glass. It was found that dust particles adhere more strongly over glass compared with activated carbon. When the glass surface was roughened, the adhesion force of dust and AC has tremendously been reduced. In another study by Darwish et al. [52] studied the effect of dust

pollutant type on PV. They highlighted a few points which were related to characteristics of dust on solar array. they found 15 types of dusts mentioned in different research including,, red soil, cement, ash, carbon, limestone, silica, calcium carbonate, sand, sand clay, soil, mud and coarser mode of air born dust, and Harmattan dust. From all this materials, six of them were found to have more significant effect on PV (ash, calcium, limestone, soil, sand and silica). They also reported that the impact of these materials on PV characteristics is limited since most of the studies considered artificial dust rather than natural dust accumulation.

4. Conclusion

Accumulation of dust particles on solar panels is a growing area of concern due to their adverse effect of photovoltaic module performance and reliability. In this work, we reported on the theoretical and experimental analysis of adhesion forces that controls the mechanism of bonding between dust and PV surfaces. Four fundamental adhesion forces were evaluated: capillary, van der Waal, electrostatic and gravitational forces. It is found that under high relative humidity, the adhesion mechanism between dust particles and PV module surfaces is dominated by capillary force with 98% share of total forces, while van der Waal force dominates under dry conditions. The effect of surface roughness over the coated vs. clean glass did not show significant decrease in the adhesion force as measured in the lab. The dominant force in the lab is van der Waal while roughness significantly affects the capillary force as the increase of surface roughness prevents the formation of a complete capillary meniscus at the particle-surface contact point and hence weakens the capillary force. Moreover, real field data for 18 months of soiling over solar panels in Qatar were investigated and resulted in proposing a novel modified sigmoid function that predicts a relative humidity inflexion value at which transition in the particulate matter deposition rate takes place from low to high values. The inflexion RH value was found to

be around 70% which is in agreement with the theoretical evaluation of our study and previous studies.

Figure Captions

Figure 1. Representative SEM micrographs with various magnifications of the dust particles collected at The Solar Test Facility.

Figure 2. Particle size distribution of the dust samples considered in this study.

Figure 3. Representative scheme of capillary force between dust particle and glass substrate.

Figure 4. Representative scheme of van der Waal force between dust particle and glass substrate.

Figure 5. Representative scheme of electrostatic force between dust particle and glass substrate.

Figure 6. Representative scheme of gravitational force between dust particle and glass substrate.

Figure 7. Red dot shows the location of the Solar Test facility where PM soiling on PV panels data was obtained. Red circle shows a 1 km radius from the Solar Test facility. Highly transited roads are highlighted in yellow.

Figure 8. Panel A shows the correlation of accumulated PM_{10} and PV PR, while panel B shows each data point colored by the daily mean RH.

Figure 9. Value of the sticky-fraction as a function of RH, the values resulting in the best fit when compared to PV Performance Ratio are shown.

Figure 10. The final correlation between sticky PM10 and Performance Ratio.

Figure 11. Diurnal variability of mean normalized deposited PM10..

Figure 12. The contact angle measured over the coated glass surface.

Figure 13. Surface roughness (RMS) of uncoated and TiO_2-coated substrates.

Figure 14. AFM tip with dust particle mounted for adhesion force measurement.

Figure 15. The average adhesion force between dust particles and coated and uncoated substrates.

References

[1] B. Aissa, R.J. Isaifan, A. Abdulla, V. Madhavan, Structural and physical properties of the desert-dust particles and their influence on the PV panels performance in Qatar, Sci. Rep. 6 (2016) 31467.

[2] M. Corn, The adhesion of solid particles to solid surfaces, I. A review, J. Air Pollut.

Control. 11 (1961) 523–528.

[3] R. Jones, H.M. Pollock, J.A.S. Cleaver, C.S. Hodges, Adhesion forces between glass and silicon surfaces in air studied by AFM : Effects of relative humidity , particle size , roughness and surface treatment ., Langmuir. 18 (2002) 8045–8055.

[4] Y. Quan, L. Zhang, R. Qi, R. Cai, Self-cleaning of Surfaces : the Role of Surface Wettability and Dust Types, Sci. Rep. 6:38239 (2016) 1–12. doi:10.1038/srep38239.

[5] S. Aramrak, M. Flury, J.B. Harsh, Detachment of deposited colloids by advancing and receding air-water interfaces, Langmuir. 27 (2011) 9985–9993.

[6] Y.I. Rabinovich, J.J. Adler, M.S. Esayanur, A. Ata, R.K. Singh, B.M. Moudgil, Capillary forces between surfaces with nanoscale roughness, Adv. Colloid Interface Sci. 96 (2002) 213–230. doi:10.1016/S0001-8686(01)00082-3.

[7] H.R. Moutinho, C. Jiang, B. To, C. Perkins, M. Muller, L. Simpson, Adhesion mechanisms on solar glass : E ff ects of relative humidity , surface roughness , and particle shape and size, Sol. Energy Mater. Sol. Cells. 172 (2017) 145–153. doi:10.1016/j.solmat.2017.07.026.

[8] A. Kay, M. Gratzel, Low cost photovoltaic modules based on dye sensitized nanocrystalline titanium dioxide and carbon powder, Sol. Energy Mater. Sol. Cells. 44 (1996) 99–117.

[9] R.J. Isaifan, A. Samara, W. Suwaileh, D. Johnson, W. Yiming, A.A. Abdallah, et al., Improved Self-cleaning Properties of an Efficient and Easy to Scale up TiO2 Thin Films Prepared by Adsorptive Self-Assembly, Sci. Rep. 7 (2017) 9466. doi:10.1038/s41598-017-07826-0.

[10] Y.Y. Quan, L.Z. Zhang, Experimental investigation of the anti-dust effect of transparent hydrophobic coatings applied for solar cell covering glass, Sol. Energy Mater. Sol. Cells. 160 (2017) 382–389. doi:10.1016/j.solmat.2016.10.043.

[11] J.H. Zhi, L.Z. Zhang, Y. Yan, J. Zhu, Mechanical durability of superhydrophobic surfaces: The role of surface modification technologies, Appl. Surf. Sci. 392 (2017) 286–296. doi:10.1016/j.apsusc.2016.09.049.

[12] R.J. Isaifan, D. Johnson, S. Mansour, A. Samara, W. Suwaileh, K. Kakosimos, Theoritical and experimental characterization of efficient anti-dust coatings under desert conditions, J. Thin Film. Res. 2 (2018) 25–29.

[13] R.J. Isaifan, M. Couillard, E.A. Baranova, Low temperature-high selectivity carbon monoxide methanation over yttria-stabilized zirconia-supported Pt nanoparticles, Int. J. Hydrogen Energy. 42 (2017) 13754–13762.

[14] R.J. Isaifan, S. Ntais, M. Couillard, E.A. Baranova, Size-dependent activity of Pt/yttria-stabilized zirconia catalyst for wireless electrooxidation of ethylene and carbon monoxide

in oxygen free environment, J. Catal. 324 (2015) 32–40.

[15] J. Goldstien, D. Newbury, P. Joy, A. Lyman, C. Lifshin, Scanning Electron Microscopy and X-Ray Microanalysis: A Text for Biologists, Material Scientists and Geologists, Plenum Press, New York, USA, 2012.

[16] D. Johnson, F. Galiano, S.A. Deowan, J. Hoinkis, A. Figoli, N. Hilal, Adhesion forces between humic acid functionalized colloidal probes and polymer membranes to assess fouling potential, J. Memb. Sci. 484 (2015) 35–46.

[17] D. Johnson, N. Hilal, W.R. Bowen, Basic principles of atomic force microscopy, Atomic force microscopy in process engineering: An introduction to AFM for improved processes and product, in: At. Force Microsc. Process Eng., IChemE, UK, 2009.

[18] W. Javed, Y. Wubulikasimu, B. Figgis, B. Guo, Characterization of dust accumulated on photovoltaic panels in Doha, Qatar, Sol. Energy. 142 (2017) 123–135.

[19] H. Al-Thani, M. Koc, R.J. Isaifan, A review on the direct effect of particulate atmospheric pollution on materials and its mitigation for sustainable cities and societies, Environ. Sci. Pollut. Res. 2018 (n.d.) 1–19.

[20] H. Al-Thani, M. Koc, R.J. Isaifan, Investigations on Deposited Dust Fallout in Urban Doha : Characterization , Source Apportionment and Mitigation, Environ. Ecol. Res. 6 (2018) 493–506. doi:10.13189/eer.2018.060510.

[21] A.D. Zimon, Adhesion of dust and powder, London, UK., 1969.

[22] B. Figgis, B. Brophy, PV Coatings and Particle Adhesion Forces, in: PV Days 2015 Proc., 2015: pp. 1–9.

[23] O. Pitois, X. Chateau, Small particle at a fluid interface: Effect of contact angle hysteresis on force and work of detachment, Langmuir. 18 (2002) 9751–9756.

[24] H.-J. Butt, M. Kappl, Normal capillary forces, Adv. Colloid Interface Sci. 146 (2009) 48–60.

[25] P. Lambert, J. Valsamis, Axial Capillary Forces, in: Surf. Tens. Microsc. Eng. Below Capill. Length, Springer, 2013: pp. 1–27. doi:10.1007/978-3-642-37552-1.

[26] M.A. Felicetti, F. Piantino, J.R. Coury, M.L. Aguiar, Influence of removal time and particle size on the particle substrate adhesion force, Brazilian J. Chem. Eng. 25 (2008) 71–82.

[27] J. Visser, Adhesion of Colloidal Particles, Surf. Colloid. Sci. 8 (1976) 3–79.

[28] L. Bergstrm, Hamaker constants of inorganic materials, Adv. Colloid. Interface Sci. 70 (1997) 125–169.

[29] P. Lambert, S. Régnier, Surface and contact forces models within the framework of microassembly, J. Micromechatronics. 3 (2006) 123–157.

[30] J.A.S. Cleaver, J.W.G. Tyrrell, The Influence of Relative Humidity on Particle Adhesion – a Review of Previous Work and the Anomalous Behaviour of Soda-lime Glass †, KONA. 22 (2004) 9–22.

[31] G. Lomboy, S. Sundararajan, K. Wang, S. Subramaniam, A test method for determining adhesion forces and Hamaker constants of cementitious materials using atomic force microscopy, Cem. Concr. Res. 41 (2011) 1157–1166.

[32] H. Choi, H. Kim, S. Hwang, C. Wonbong, M. Jeon, Dye-sensitized solar cells using graphene-based carbon nano composite as counter electrode, Sol. Energy Mater. Sol. Cells. 95 (2011) 323–325.

[33] A. Rifai, N.A. Dheir, B.S. Yilbas, M. Khaled, Mechanics of dust removal from rotating disk in relation to self-cleaning applications of PV protective cover, Sol. Energy. 130 (2016) 193–206.

[34] C. Tan, S. Gao, B. Wee, A. Asa-Awuku, B. Thio, Adhesion of Dust Particles to Common Indoor Surfaces in an Air-Conditioned Environment Adhesion of Dust Particles to Common Indoor Surfaces in an Air-Conditioned Environment, Aerosol Sci. Technol. 6826 (2014) 541–551. doi:10.1080/02786826.2014.898835.

[35] Y.I. Rabinovich, T.G. Movchan, N.V. Churaev, P.G. Ten, Phase-separation of binary mixtures of polar liquids close to solid surfaces, Langmuir. 7 (1991) 817–820.

[36] J. Visser, Particle adhesion and removal: a review., Part. Sci. Technol. 13 (1995) 169.

[37] M. Gauthier, S. Alvo, J. Dejeu, B. Tamadazte, P. Rougeot, S. Regnier, Analysis and specificities of adhesive forces between microscale and nanoscale, in: IEEE Trans. Autom. Sci. Eng., 2013: pp. 1–9.

[38] R.A. Bowling, An Analysis of Particle Adhesion on Semiconductor Surfaces, J. Electrochem. Soc. 157 (1985) 2208–2214.

[39] F.L. Leite, C.C. Bueno, A.L. Da Róz, E.C. Ziemath, Theoretical Models for Surface Forces and Adhesion and Their Measurement Using Atomic Force Microscopy, 2012. doi:10.3390/ijms131012773.

[40] B. Gady, Measurement of interaction forces between micometer-sized particles and flat surfaces using an Atomic Force Microscope, Purdue University, 1996.

[41] L. V Deputatova, V.S. Filinov, D.S. Lapitsky, V.Y. Pecherkin, R.A. Syrovatka, L.M. Vasilyak, et al., Measurement of the charge of a single dust particle, J. Pysics. 653 (2015) 1–5. doi:10.1088/1742-6596/653/1/012129.

[42] J.R. Cozens, R.A. Syms, Optical Guided Waves and Devises, Mc Graw-Hill, Berkshire,

England, 1992.

[43] J.A.S. Cleaver, J.W.G. Tyrrell., The Influence of Relative Humidity on Particle Adhesion, Kona Powder Part. 22 (2004) 9.

[44] H. Kweon, S. Yiacoumi, C. Tsouris., The role of electrostatic charge in the adhesion of spherical particles onto planar surfaces in atmospheric systems., Colloids Surfaces A Physicochem. Eng. Asp. 481 (2015) 583–590.

[45] V.B. Menon., Particle Adhesion to Surfaces: Theory of Cleaning. Printed in: R.P. Donovan, Particle Control for Semiconductor Manufacturing, CRC Press LLC, 1990.

[46] B. Figgis, A. Nouviaire, Y. Wubulikasimu, W. Javed, B. Guo, A. Ait-Mokhtar, et al., Investigation of factors affecting condensation on soiled PV modules, Sol. Energy. 159 (2018) 488–500. doi:10.1016/j.solener.2017.10.089.

[47] V.A. Ganesh, A.S. Nair, H.K. Raut, T.M. Walsh, S. Ramakrishna, Electrospun SiO2 nanofibers as a template to fabricate a robust and transparent superamphiphobic coating, R. Soc. Chem. Adv. 2 (2012) 2067.

[48] J.A. Pimenoff, A.K. Hovinen, M.J. Rajala, Nanostructured coatings by liquid flame spraying, Thin Solid Films. 517 (2009) 3057–3060.

[49] R. Fateh, A.A. Ismail, R. Dillert, D.W. Bahnemann, Highly active crystalline mesoporous TiO2 films coated onto polycarbonate substrates for self-cleaning applications, J. Phys. Chem. C. 115 (2011) 10405.

[50] M. Gotzinger, W. Peukert, Particle Adhesion Force Distributions on Rough Surfaces, Langmuir. 20 (2004) 5293–5303.

[51] S. Chen, B. Zhang, X. Gao, Z. Liu, X. Zhang, Direction Dependence of Adhesion Force for Droplets on Rough Substrates, Langmuir. 33 (2017) 5298–5303.

[52] Z. Darwish, H. Kazem, K. Sopian, M. Al-Goul, H. Alawadhi, Effect of dust pollutant type on photovoltaic performance, Renew. Sustain. Energy Rev. 41 (2015) 735–744.

Acknowledgement

We acknowledge financial support from Qatar Environment and Energy Research Institute (QEERI), at Hamad Bin Khalifa University-Qatar Foundation (Doha, Qatar). Authors would like to thank Eng. Wafa Suwaileh for taking the SEM images of dust particles, Dr. Ahmed Fard for measuring the density of the dust samples and Dr. Tarik Rhadfi for TiO_2 nanocolloid synthesis.

Author Contributions

R. I. helped with TiO_2 nanocolloid synthesis, performed the coating of the samples, conducted theoretical calculations of the adhesion forces, data analysis and writing the article. D. J. performed AFM measurements for the roughness of the films and the adhesion force. L.A. performed PM_{10} and meteorological measurements, and developed the soiling model described in section 3.3. B.F. calculated the PV Performance Ratio used for the development of the soiling model. M.A. provided technical support for the project.

Additional Information

Competing financial interests: The authors declare no competing financial interests.